Oriental Journal of Chemistry Vol. **25**(1), 01-07 (2009)

Selective photolysis of aqueous colloidal nano-particles of some metal- oxide semiconductors for hydrogen generation

KASEM K. KASEM

Nat. Inform. Math. Sciences department, School of Art and Science
Indiana University Kokomo, Kokomo, IN, 46904 (USA)

(Received: January 01, 2009; Accepted: February 09, 2009)

ABSTRACT

Aqueous solutions of $[Fe(CN)_6]^{4-}$ containing nano-particles of p-type Fe_2O_3, or TiO_2 doped with V_2O_5, or Cu_2O were used for photo dissociation of water for the selective production of hydrogen. The effects of some oxo-anions were investigated. Studies show that Fe_2O_3 doped with ZnO was more efficient than Fe_2O_3 doped with MgO. Potassium ferro-cyanide gives the most promising results as a solvated-electron supplier and electron exchanger in basic borate buffer. Our studies show that the maximum hydrogen production was recorded for TiO_2 doped with V_2O_5 oxide in basic tartarate buffer. Aqueous nano systems used in these studies retained their stability as indicated by the reproducibility of their photo-catalytic activities.

Key words: Selective photolysis, nano-particles, metal- oxide semiconductors.

INTRODUCTION

Photochemical cleavage of water into hydrogen and oxygen using powder suspensions of some semiconductors was reported by several researchers[1-11] for examples. Most of the studies on the photo-dissociation of water were done over compact semiconductor electrodes. Colloidal semiconductors were used because of their larger surface area and their ability to carry out all reactions that previously associated with massive semiconductor electrodes. In particular systems, platonized semiconductors powder such as TiO_2 was used for simultaneous production of oxygen and hydrogen. Several methods were used to generate ordered assemblies of narrow band gap semiconductor nanostructures for harvesting visible-light energy. In most of these methods, one material with a specific band gap is being produced. Some studies[12-20], performed on metal chalcogenides such as sulfides, selenides, tellurides, reported low conversion efficiencies. The photocurrent obtained using such nano-particle assemblies is often low because fast charge recombination limits photocurrent and consequently hydrogen generation.

Hydrated electrons (e_{aq}^-) can play an important role in the photodissociation of water through this reaction:

$$e_{aq}^- + e_{aq}^- = H_2O + 2OH^- \quad ...(1)$$

This reaction proceeds with a rate $k \approx 1\times10^{10}$ M^{-1} sec^{-1} [21]. The molecular orbital structure of hexacyano iron (II) $[Fe(CN)_6]^{4-}$ allows electronic transition under the photo excitation condition and the reaction produces hydrated electrons that reacts according to the above reaction. At the same time, $[Fe(CN)_6]^{4-}$ undergoes oxidation to $[Fe(CN)_6]^{3-}$. The oxidation process

compromises the reported high rate. The disadvantage of homogeneous process for hydrogen production is its irreversibility. However, such disadvantage can be overcome through the use of semiconductor system which acts as an electron donor and reduces $[Fe(CN)_6]^{3-}$ back to $[Fe(CN)_6]^{4-}$. Achieving such goal will create the conditions of reversible ergo-dynamics. The conditions could be reached if the rate of reduction of $[Fe(CN)_6]^{3-}$ could be equated to that of the rate of formation of hydrated electrons from $[Fe(CN)_6]^{4-}$.

p-type semiconductors particles can be used for the heterogeneous reduction of hydrogen ions to generate hydrogen if a suitable hole-scavenger is present in the suspension media. With the high rate of photo-generation of hydrated electrons in homogenous solutions, it is possible that hydrogen can be generated heterogeneously and homogeneously by the photolysis of colloidal particles suspended in ferro-cyanide solutions at room temperature.

In this paper, we highlight the use of p-type Fe_2O_3 colloidal nano particles doped with either ZnO or MgO, and p-type TiO_2 doped with V_2O_5 or Cu_2O to study the rate of hydrogen production during the photolysis of ferro-cyanide solutions using visible light photons. The possibility of using these systems in solar energy based photolysis cell that achieve the goal of reversible cyclic, efficient process for hydrogen production is explored.

EXPERIMENTAL

Reagents

All reagents were of analytical grade. Iron (III) oxide doped with either Mg or Zn oxides to form $Fe_{1.8}Mg_{0.2}O_3$, or $Fe_{1.9}Zn_{0.1}O_3$ were prepared following procedures published by F.J. Berry et al (22). Titanium Oxide TiO_2 doped with V_2O_5 was prepared as described elsewhere (23) using $NaVO_3$ and $TiCl_3$ as starting materials.

Instrumentation

BAS 100W electrochemical analyzer (Bioanalytical Co.) was used to perform the electrochemical studies. Steady state reflectance spectroscopy were performed using Shimadzu UV-2101 PC. An Olympus BX-FLA60 reflected light Fluorescence Microscope working with polarized light was used to determine the particle size of colloidal particles.

Photolysis cell

The electrolysis cell was one compartment a Pyrex cell with quartz window facing the irradiation source. The working electrode, a 10-cm^2 platinum gauze cylinder, and had a solution volume of 100 mL. Suspensions were stirred with a magnetic stirrer during the measurements. An Ag/AgCl/Cl^- reference electrode was also fitted in this compartment. A 10-cm^2 platinum counter- electrode was housed in a glass cylinder sealed in one end with a fine porosity glass frit.

Irradiations were performed with a solar simulator 300 watt xenon lamp (Newport) with an IR filter. The measured photo current was normalized considering two photons per one hydrogen molecule, and used to calculate the number of moles of hydrogen generated per square meter per hour of illumination. A Flame test was used to confirm that the gas bubbles generated upon irradiation were hydrogen.

RESULTS AND DISCUSSIONS

Band-energy map of the studied oxides Doped Iron(III) Oxide

Steady state reflectance spectra of the colloidal nano-particles (100 nm) of Fe_2O_3 doped with either MgO or ZnO are shown in Fig. 1. The sudden drop in absorption curves appeared around 570-590 nm. This reflect a band gap of H"2.2 eV. Although these dopants did not affect the height of the band gap, they did affects the iron (III) oxide direct and indirect band transitions. Furthermore, the replacement of two Fe^{3+} by two of either Mg^{2+} and Zn^{2+} causes linear structure deformation that grant p-type nature of Fe_2O_3 oxide particles.

The effects of the doping can be identified after treatment of the steady state reflection spectra of Fe_2O_3 doped with either MgO or ZnO, shown in Fig. 2. The following equations (24) can be used to determine whether direct or indirect transition band structures exist in these doped oxides:

$$(\alpha E_\gamma)^2 \propto E_\gamma - E_{gd} \quad ...(2)$$

$$\alpha \propto \frac{(E_\gamma + E_p - E_g)^2}{e^{(E\gamma/KT)} - 1} + \frac{(E_\gamma + E_p - E_g)^2 e^{(Eg/kT)}}{e^{(E\gamma/KT)} - 1} \quad ...(3)$$

Where a is absorption coefficient, E_g is the optical band gap.

The plot of $\alpha^{½}$ vs E_g will lead to identification of indirect bands transitions , while the plot of $(\alpha E_g)^2$ vs E_g will allow the determination of the direct transitions. These plots are known as Tauc plots. The results of these treatments are displayed in Fig. 2 A&B. from which we can identify the following quantities for the direct and indirect band transitions in the studied oxides. For Fe_2O_3 doped with MgO or Fe_2O_3 doped with ZnO Figure 2 shows that the intercept of the linear portion of the $\alpha^{½}$ vs E_g with x axe gives H≈ 2.3 eV for the indirect band transition, while that of $(\alpha E_g)^2$ vs E_g gave ≈ 1.9 eV for the direct band transitions. The fact that doping iron oxide with greater band gap material such as ZnO or MgO results in a doped Fe_2O_3 oxide with band gap greater than that of pure Fe_2O_3. This is not the case as shown by $(\alpha E_g)^2$ vs E_g plot., as 1.90 eV is much less than the band gap expected band gap of pure Fe_2O_3 (≈2.2 eV). Such results indicate that these doped oxides possess an indirect band transition, which is in agreement with the reported studies[25,26].

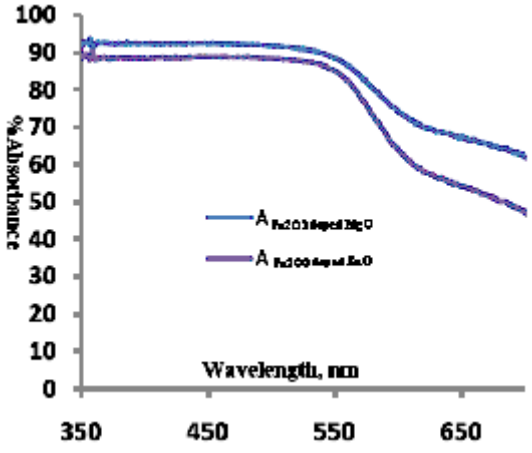

Fig. 1: Steady state reflectance spectra for Fe_2O_3 doped with MgO and with ZnO

Doped TiO_2

Similar studies were performed on TiO_2 doped with 10 % V_2O_5

The results indicates that an indirect band gap of Eg ≈ 2.8 eV, this is greater than the direct band gap with a value of Eg ≈ 2.5 eV, which is unlikely to be the accurate value of the band gap of the doped TiO_2. This suggests that TiO_2 has an indirect band gap transition when doped with V^{+5}. It is known that the depletion layer width decreases with increasing distance of the energy level of the doping material from the conduction band. The V, Zn, Mg oxides dopants energy levels are not located far further from the conduction band of TiO_2. This increases the depletion layer width and consequently enhances charge transfer at the TiO_2 / electrolyte interface.

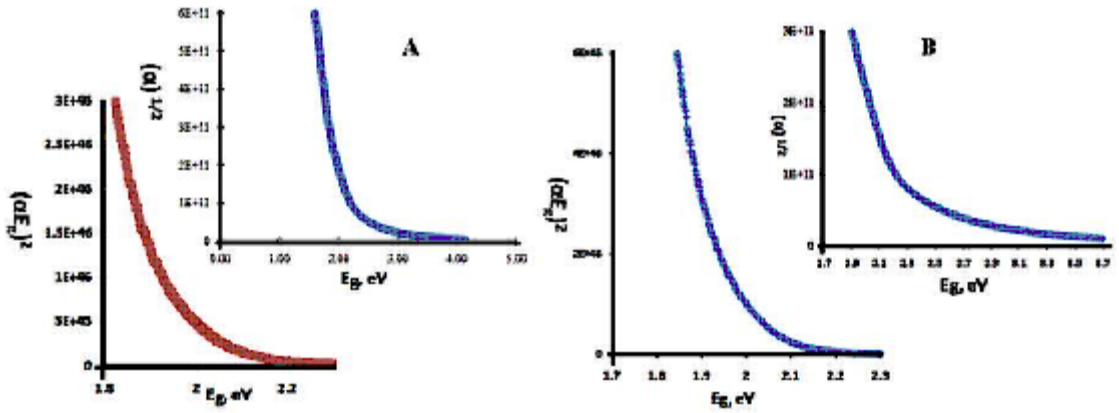

Fig. 2: Tauc plots for A- Fe_2O_3 doped with MgO B- Fe_2O_3 doped with ZnO

It is well known that for an indirect transition, three entities are needed to interact in order to proceed; an electron, a photon, and a phonon. Such interaction with these three entities makes the indirect transition take place at much slower rate than direct transition. This also causes the electron-hole recombination process to be much slower than that in indirect transition band gap. This is because electron–hole recombination process has to be mediated by the phonons. We anticipate that the photonic process at the interfaces of these doped oxides suspensions will enhance the photo-conversion efficiencies.

Photolysis of aqueous doped oxides nano-particles colloidal solutions

Photolysis of p-Type Fe_2O_3

Doping of Fe_2O_3 with either MgO or ZnO, results in formation of a p-type iron oxide semiconductor. In presence of a hole-scavenger such as tartarate or borate the photolysis process became selective towards generation of hydrogen only. Furthermore, as mentioned above, the dopants caused indirect band transitions. The magnitude of such indirect transitions can have a direct effect on the photonic responses of these doped iron (III) oxides.

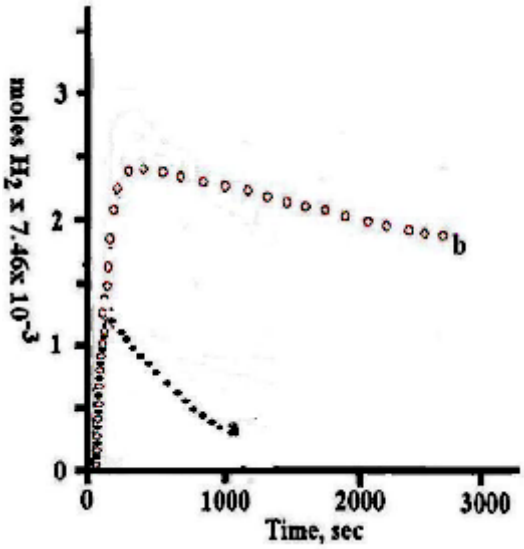

Fig. 3: Rate of hydrogen production upon photolysis of colloidal nano-particles of Fe_2O_3 doped with ZnO) borate buffer. a) 10 mM of $K_4[Fe(CN)_6]$ in 0.2M borate buffer (pH=10) , b) 10 mM of $K_4[Fe(CN)_6]$ in 0.2M borate buffer (pH=10) containing Fe_2O_3 doped with ZnO

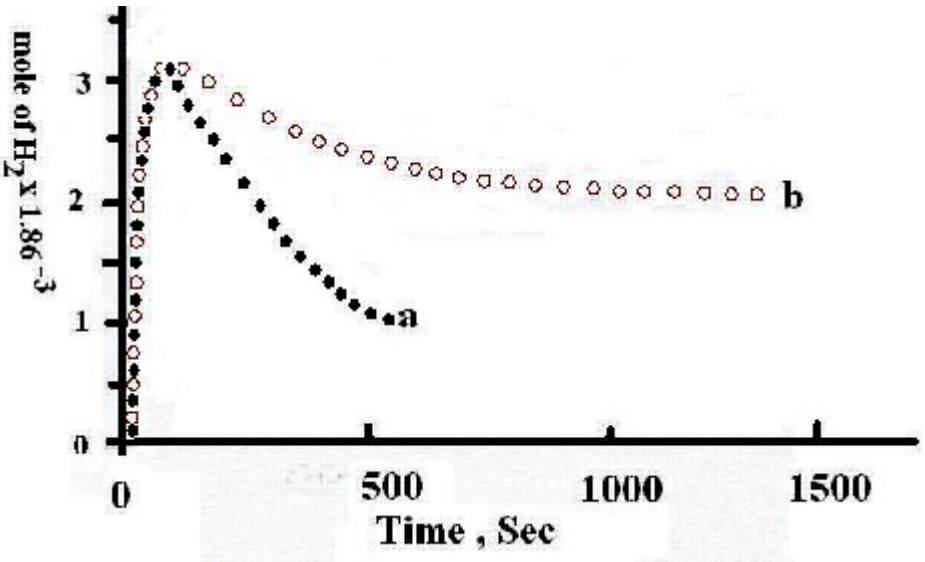

Fig. 4: Rate of hydrogen production upon photolysis of colloidal nano-particles of Fe_2O_3 doped with MgO borate buffer. a) 10 mM of $K_4[Fe(CN)_6]$ in 0.2M borate buffer (pH=10) , b) 10 mM of $K_4[Fe(CN)_6]$ in 0.2M borate buffer (pH=10) containing Fe_2O_3 doped with MgO

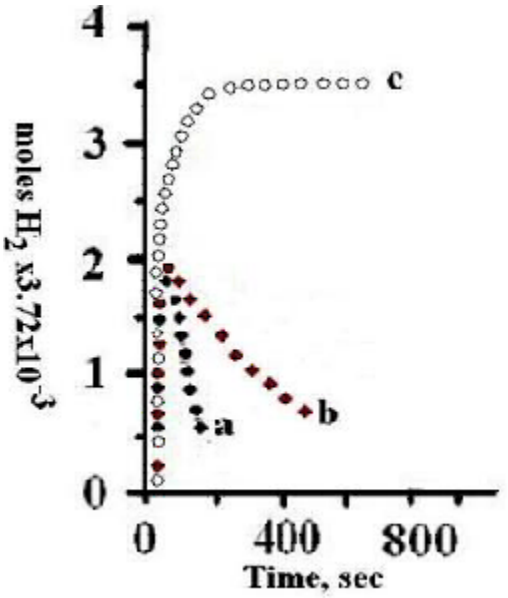

Fig. 5: Rate of hydrogen production upon photolysis of colloidal nano-particles of TiO_2 doped with V_2O_5 borate buffer. a) 10 mM of $K_4[Fe(CN)_6]$ in 0.2M borate buffer (pH=10) , b) 10 mM of $K_4[Fe(CN)_6]$ in 0.2M borate buffer (pH=10) doped TiO_2 doped with 5% V_2O_5. c) 10 mM of $K_4[Fe(CN)_6]$ in 0.2M borate buffer (pH=10) containing TiO_2 doped with 10 % V_2O_5

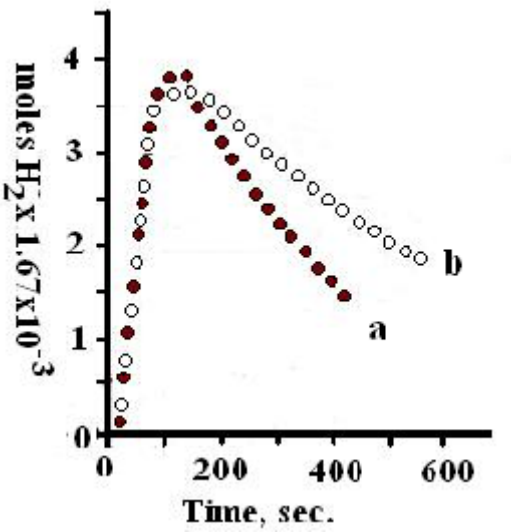

Fig. 6: Rate of hydrogen production upon photolysis of colloidal nano-particles of Cu_2O in borate buffer. a) 10 mM of $K_4[Fe(CN)_6]$ in 0.2M borate buffer (pH=10), b) 10 mM of $K_4[Fe(CN)_6]$ in 0.2M borate buffer (pH=10) containing Cu_2O

Photolysis of aqueous $[Fe(CN)_6]^{4-}$ results in formation of hydrated electrons e_{aq}^- and oxidation to $[Fe(CN)_6]^{3-}$ according to the following equation:

$$[Fe(CN)_6]^{4-} + h\nu = [Fe(CN)_6]^{3-} + e_{aq}^- \quad ...(4)$$

Due to the irreversible nature of this reaction, when all the $[Fe(CN)_6]^{4-}$ is oxidized to $[Fe(CN)_6]^{3-}$ hydrated electrons are no longer generated. To reverse such process, illumination of doped iron (III) oxide particles (´) in presence of hole-scavenger (X^{2-}) such as borate $B_4O_7^{2-}$, tartarate $K[C_2H_2(OH)_2(COO)_2]^{2-}$,or phosphates HPO_4^{2-}, reduction of $[Fe(CN)_6]^{3-}$ is possible as represented by this reaction:

$$\bullet + h\nu + X^{2-} + [Fe(CN)_6]^{4-} = X_5^{3-} + [Fe(CN)_6]^{3-} \quad ....(5)$$

The rate of reaction 4 is greater than that of reaction 5 due to the heterogeneity factor and the nature of the indirect band transitions of the semiconductor oxide particles. Co-existence of doped p-type iron (III) particles with ferro-cyanide anions under illumination allows continuity in production of hydrogen. This can be identified by preventing the photocurrent from dropping back to lower quantities after reaching the maximum value. This will be the criterion by which the comparison between one oxide with others is made. Photolysis of aqueous colloidal solutions of Fe_2O_3 doped with ZnO and with MgO in presence of 10 mM of $K_4[Fe(CN)_6]$ in 0.2M borate buffer (pH=10) is displayed in Figures 3 and 4 respectively . It is quite clear that doping iron (III) oxide with ZnO results in better photo-conversion of absorbed light. This can be noticed by comparing traces b in both figures.

Photolysis of aqueous colloidal TiO_2 Doped with 10% V_2O_5

The objective of doping TiO_2 with V_2O_5 is to create a metal oxide assembly capable of electron-hole production when illuminated with visible light. Figure 5 shows that adding colloidal nano-particles results in a better rate in hydrogen production (trace b) than that in basic borate buffer containing $K_4[Fe(CN)_6]$ (trace a). However, when TiO_2 doped with 10% V_2O_5 is used, a greater hydrogen production rate is observed (trace c). Such behavior was expected because with TiO_2 only, the high band gap (3.3 eV) allows only UV light with $\lambda <$ 400 nm to be absorbed. As the intensity of UV in the solar simulator used in this study is low, a corresponding small photonic activity of the suspended nano-particles during the illuminations is expected. However, the photocurrent of the TiO_2 doped with V_2O_5 was greater than that of TiO_2. This can be attributed to 1- the high surface state density introduced by the diffusion of vanadium ions (25), 2- decreasing the rate of electron –hole recombination due to the change of the band transition mechanism from direct to indirect.

Photolysis of aqueous colloidal Cu_2O

Photolysis of pure Cu_2O suspensions in aqueous borate buffer of pH =10, generates much less hydrogen production rate compared to the other oxides, the results are displayed in Figure 6 (trace a and b). This low production rate is due to the lack of dopants that decreases the electron-hole recombination rate. It is well known that for illuminated Cu_2O, three possible ways for the generated electron-hole pairs to be consumed, 1- is the recombination of electron-hole, 2-, is electron transfer to other chemical agent, and 3- is the reduction of Cu^+ ions to metallic copper. The fact that the photochemical behavior of Cu_2O was reproducible for several times, suggests that the reduction of Cu^+ did not take place during the photolysis process under operation conditions.

Table 1: Steady state photo-current for studied metal oxides nano-particles at pH =10 in different polyatomic anions (hole scavengers)

Anion	Photo-current, A/ m^2		
	Fe_2O_3 (MgO)	Fe_2O_3 (ZnO)	TiO_2 (10%)V_2O_5
Citrate $K[C_3H_4(OH)(COO)_3]^{2-}$	0.620	0.200	1.10
Tartarate $K[C_2H_2(OH)_2(COO)_2]^{2-}$	1.00	2.70	0.90
Borate $(B_4O_7)^{2-}$	0.300	0.510	0.62
Phosphate $(HPO_4)^{2-}$	1.400	2.40	1.30

Hole-scavenger Effects

Results recorded in table 1 do not show specific advantages of one poly-anion type over the other, however it is quite noticeable that phosphate gives the greatest photo-current with all of the studied oxides under operation conditions. More details studies are needed to explain such behavior, and correlate the photonic behavior with certain property of the poly-anion species.

CONCLUSION

The observed better photonic responses of the doped iron (III) oxide doped with ZnO or with MgO and TiO_2 doped with V_2O_5 than the native ones can be attributed to the fact that dopants: 1- facilitate the transfer of charge carriers at the interface because of the increased flat-band potential, and 2- increase the absorption of incident light energy as a result of the increase in the depletion layer width at the junction (26).

ACKNOWLEDGMENTS

This work was supported by Indiana University Summer faculty fellowship program

REFERENCES

1. C. J. Sartoretti, B. D. Alexander, R. Slarska, I. A. Rutkowska, J. Augustynski, and R. Cerny, *J. Phys. Chem.,* B, **109**: 13685 (2005).
2. C. J. Sartoretti, M. Ulmann, B. D. Alexander, B.D Augustynski, *J. Chem. Phys. Lett.*, **376**: 194 (2003).
3. T. Lindgren, L. Vayssieres, H. wang, and S.E. Lindquist, *Chem. Phys. Nanostruct. Semicond,* **83**: 110 (2003)
4. K. Sayama and H. Arakawa, *J. Phys.Chem.*, **97**: 531(1993).
5. Y. Inoue, Y. Asai and K. Sato, *J. Chem. Soc., Faraday T rans*. 90: 797 (1994).
6. S. Tabata, H. Nishida, Y. Masaki and K. Tabata*, Catal. Let*. **34**: 245 (1995).
7. A. M. Linsebigler, G. Lu and J. T. Yates, Jr., *Chem. Rev*. **95**: 735 (1995).
8. A. J. Bard and M. A. Fox, Acc. *Chem. Res.* **28**: 141 (1995).
9. T. Takata, Y. Furumi, K. Shinohara, A. Tanaka, M. Hara, J. N. Kondo and K. *Domen, Chem. Mater*. **9**: 1063 (1997).
10. K. Yamaguti, and Shinri Sato, *J. Chem. Soc, faraday Trans*. 1: 81, 1237 (1985).
11. A. Mills, and G. Porter, J. chem. *Soc, faraday Trans*. 1 1982, 78 , 3659 (1982).
12. Graetzel, M. *Nature* **414**: 338(2001).
13. Graetzel, M., Nanocrystalline electronic junctions. In *Semiconductor Nanoclusters - Physical, Chemical and Catalytic Aspects*; Kamat, P. V Meisel, D., Eds.; Elsevier Science: Amsterdam, 353 (1997).
14. K. R. Goidas , M. Bohorques, and Kamat, *J. Phys. Chem.* B**94**: 6435(1990)
15. Vogel, R.; Pohl, K.; Weller, H. *Chem. Phys. Lett.* **174:** 241 (1990).
16. Kohtani, S.; Kudo, A.; Sakata, T. *Chem. Phys. Lett.* **206**: 166(1993).
17. Vogel, R.; Hoyer, P.; Weller, H. *J. Phys. Chem.* **98**: 3183 (1994).
18. Plass, R.; Pelet, S.; Krueger, J.; Gratzel, M.; Bach, U. *J. Phys. Chem.* B**106**: 7578 (2002).
19. Peter, L. M.; Wijayantha, K. G. U.; Riley, D. J.; Waggett, J. P. *J. Phys.Chem.* B**107**: 8378 (2003).
20. Liu, D.; Kamat, P. V. *J. Phys. Chem.* **97**: 10769 (1993).
21. S. Gordon, E.J. Hars, M.S. Matheson, J. Rahani, and J. K. Thomas, *J. Am. Chem. Soc*, **85**: 1375(1963).
22. F.J.Berry, A. Bohorquez , C. Greaves , J. McManus, E. A. Moore and M. Mortimer, *J. Solid stste chemistry,* **140**: 428 (1998).
23. A. Ookubo, E. Kanezaki, and K. Ooi, Langmuir, **6**: 205 (1990).
24. Robert A, Van leeuwen, Chen-jen Hung , Danlel R. Kammler, and Jay A. Switzer. *J. Phys. Chem,* 99 15247 (1998).
25. Zhao G. Kozuka H. Lin H. Yoko T. *Thin solid films* **340**: 125 (1999).
26. Saroj Kumari, Chanakya Tripathi, Aadesh P. Singh1, Diwakar Chauhan2, Rohit Shrivastav, Sahab Dass & Vibha R. Satsangi, *Current science.* **91**(8): 1062 (2006).